2013 IEEE/RSJ International Conference on
Intelligent Robots and Systems (IROS)
November 3-7, 2013. Tokyo, Japan

Master / Slave Control of Flexible Instruments for Minimally Invasive Surgery

Antonio De Donno, Florent Nageotte, Philippe Zanne, Lucile Zorn and Michel de Mathelin

Abstract— **STRAS is a flexible robotic system based on the Anubis® platform from Karl Storz and is aimed for intraluminal and transluminal procedures. It is composed of three cable-driven sub-systems, one endoscope and two insertable instruments. The bending instruments have three degrees of freedom and can be teleoperated by the user via two commercial master interfaces (Omega.7, Force Dimension) . In this paper we investigate several ways to map the motions from the master side to the instruments, from joint per joint control to cartesian control. We describe these mappings and compare them in elementary tasks in an attempt to analyze how non-linearities affect the accuracy of control. Results show that joint control and pseudo-cartesian control provide equivalent accuracy but with different difficulties for the user.**

I. Introduction

Recently, flexible systems have been used for performing minimally invasive surgical procedures in intraluminal, transluminal or single port access operations. Multiple surgical platforms have been developed by companies and by laboratories for improving the capability of these flexible systems by providing instruments bending and triangulation [1], [2]. However, the high number of Degrees of Freedom (DoFs) to be controlled requires several surgeons to cooperate in a small working area. Robotics is probably an interesting tool for improving the use of flexible systems in minimally invasive surgery [3]. In this context we have developed a telemanipulated robotic system for assisting surgeons in intraluminal and transluminal procedures [4] (see Fig. 1). This system is based on the Anubis® platform by Karl Storz. We have previously shown [4] that it is possible for a single user to control all DoFs of the robotic system and to perform complex tasks, which necessitate two or more persons with the manual system. However, the control modality initially offered is based on joint per joint control, which is demanding for the user, who must mentally construct the elementary displacements required for obtaining the desired operational motion. In this paper we investigate different approaches for mapping motions performed on commercial master interfaces (omega.7, Force Dimension) to the slave instruments.

The instruments of the slave robot are long (80 cm) flexible cable driven systems, which introduces important non linearities and difficulties to obtain accurate models [5] [6]. The architecture is quite similar to the one of catheters [7], but the demand on velocity and reactivity is much higher. Some solutions have been proposed to control these systems in closed loop, using external sensors such as magnetic sensors [8] or the endoscopic camera [9]. But these solutions are not applicable in vivo yet. Non linearities are dependent on numerous parameters [10] and the solutions to compensate them also rely on the use of an external sensor [10]–[12].

In this work, we have chosen to control the system in open-loop, letting the user close the operational loop using the visual feedback provided by the endoscopic camera. This approach has been used in other flexible systems [13], [14]. However, for our robotic system the choice of mapping between master interfaces and the slave system has a very large influence because of two particularities: a) Each instrument has only three DoFs and, therefore, orientation and position are linked in a non intuitive way; b) A singularity in the straight position makes the system non holonomic in this configuration. We have tested four different manners to map the motion of the master interface to the slave instrument, from joint control to cartesian control.

In the following, we first give an overview of the robotic system and we present the models of the system and detail its peculiarities for control. Section III presents the master/slave mappings that have been assessed. Section IV provides additional details on the handling of singularities for cartesian approaches. Experimental results obtained for three different tasks are presented and discussed in section V.

The mechanical architecture of STRAS has been previously presented in [4] together with first manipulation experiments using joint per joint control only. This paper presents, for the first time, higher level master-slave mappings based on a kinematic modeling of the instruments, it provides objective comparisons and discuss them. The proposed mappings and the results are of interest for telemanipulated systems with standard master interfaces and ”catheter-like” slave systems.

II. Slave robotic system

The slave robotic system (called STRAS, for **S**ingle **A**ccess and **T**ransluminal **R**obotic **A**ssistant for **S**urgeons) is built on the Anubis® platform from Karl Storz. This system consists of three flexible, cable-driven sub-systems [4]: one main endoscope and two lateral flexible instruments. The endoscope carries the endoscopic camera at its tip and has two lateral channels which are deviated from the main direction by two flaps at the distal extremity. The instruments

Authors are with ICube, University of Strasbourg, CNRS - Strasbourg, France. Contact: Nageotte@unistra.fr

This work was supported by French state funds managed by the ANR within the Investissements d’Avenir programme (Labex CAMI) under reference ANR-11-LABX-0004.

Authors wish to thank KARL STORZ GmbH & Co. KG, Tüttlingen for providing the Anubis® platform and the flexible instruments and for their technical support. They also wish to thank surgeons at the IRCAD for the medical advices.

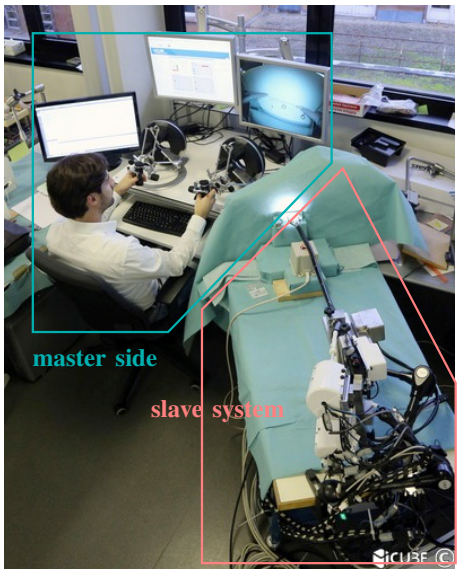

Fig. 1. STRAS is a telemanipulated system for intraluminal surgery. The slave part (right), based on the Anubis® platform, has motorized 9DoFs.

have bending extremities (one direction) and can be inserted inside the channels of the endoscope.

This system has a tree-like architecture and the DoFs of the endoscope act upon the position and orientation of the instruments (see Fig. 2) Two kinds of instruments can be used: electrical instruments and mechanical instruments.

The robot is aimed at being teleoperated once the whole system has been manually brought to the operation area.

Overall, the slave system has 9 motorized DoFs. The main central scope, which carries the endoscopic camera, can be deflected in two orthogonal directions, which allow to move the endoscopic view respectively from left to right and from up to down. Each instrument has three DoFs: translation (t_z) and rotation (θ_z) in the endoscope channel, and deflection of the active extremity (angle β). The deflection is actuated by cables running through the instrument body from the proximal part up to the distal end. Moreover, the mechanical instruments can be opened and closed.

Since the only feedback provided to the user is the endoscopic image, it is suitable to provide control of the instruments in a frame attached to the endoscopic camera.

A. Mathematical models of the instruments

In this section we present the models used for controlling the instruments. They are purely geometrical and based on usual assumptions for continuum systems [7]. They do not take into account known but complex non linear behaviors, such as cable slacking and tension loss due to friction [6]. The position of the tip of the instrument in a frame attached to the exit of the endoscope channel can be expressed in function of the actuated DoFs $q_{sl} = (\beta, \theta_z, t_z)$ as:

$$ {}^{ch}P = \begin{bmatrix} X \\ Y \\ Z \end{bmatrix} = \begin{bmatrix} (\frac{L}{\beta}(1-cos(\beta))+dsin(\beta))cos(\theta_z) \\ (\frac{L}{\beta}(1-cos(\beta))+dsin(\beta))sin(\theta_z) \\ \frac{L}{\beta}sin(\beta)+t_z+dcos(\beta) \end{bmatrix} \quad (1) $$

for $\beta \neq 0$ and ${}^{ch}P = [0;0;L+d+t_z]$ for $\beta = 0$, where L is the length of the bending section and d the length of the rigid part at the tip of the instrument.

The orientation of the tip is given by the rotation matrix between $\mathscr{F}_{ch}$ and $\mathscr{F}_{inst}$: ${}^{ch}R_{inst} = R_z(\theta_z)R_x(\beta)$. When $\beta = 0$, ${}^{ch}P$ is independent of θ_z, while ${}^{ch}R_{inst}$ is a rotation of axis z and angle θ_z. Hence, when the deflection is null it is possible to orient the instrument freely around its axis. When $\beta \neq 0$, ${}^{ch}P$ and ${}^{ch}R_{inst}$ are coupled. We have chosen to focus on the control of the position of the tip of the instrument, the orientation being obtained as a side effect.

The transformation between $\mathscr{F}_{ch}$ and $\mathscr{F}_{cam}$ is known and one easily obtain the position ${}^{cam}P = (X_{sl}, Y_{sl}, Z_{sl})^T$ of the tip of the instrument in the camera frame.

The jacobian, which relates joint velocities $\dot{q_{sl}}$ to the linear velocity of the tip of the instrument ${}^{ch}\dot{P}$ expressed in $\mathscr{F}_{ch}$ (${}^{ch}\dot{P} = J\dot{q_{sl}}$), can be written as

$$ J(q_{sl}) = \begin{bmatrix} \frac{\partial X}{\partial \beta} & -Y & 0 \\ \frac{\partial Y}{\partial \beta} & X & 0 \\ \frac{\partial Z}{\partial \beta} & 0 & 1 \end{bmatrix} \text{ for } \beta \neq 0. \quad (2) $$

For the straight positions ($\beta = 0$) it can be obtained by a second-order development of the previous expression:

$$ J(0, \theta_z, t_z) = \begin{bmatrix} cos(\theta_z)(\frac{L}{2}+d) & 0 & 0 \\ sin(\theta_z)(\frac{L}{2}+d) & 0 & 0 \\ 0 & 0 & 1 \end{bmatrix}. \quad (3) $$

B. Singularities

The determinant of J, noted Δ, is null for $\beta = 0$. The angle θ_z has then no effect on the position of the tip of the instrument (second column of the jacobian is null). Hence P can only be moved in the current plane of curvature of the instrument, *i.e.* the system is non-holonomic for this configuration.

If $\beta \neq 0$, $\Delta = \frac{\partial X}{\partial \beta}X + \frac{\partial Y}{\partial \beta}Y = \frac{\partial (X^2+Y^2)}{\partial \beta}$ is independent of t_z and θ_z. Another singularity appears when $\frac{\partial (X^2+Y^2)}{\partial \beta} = 0$, *i.e.* when the tip of the instrument is at the maximum distance from the axis of the workspace (see Fig. 4). With the actual values of $L = 18.4mm$ and $d = 15.2mm$ the singularity appears for $\beta_{sing} = 101.77°$. Then

$$ J = \begin{bmatrix} 0 & -Y & 0 \\ 0 & X & 0 \\ \frac{\partial Z}{\partial \beta} & 0 & 1 \end{bmatrix}, \text{ and at this singularity there is} $$

hence redundancy of motion along the Z axis which can be obtained using either t_z or β.

C. Inverse position kinematic model

For cartesian and pseudo-cartesian control modalities (see section III-B), it is necessary to invert the kinematic position model because the loop is not closed at the operational level. No closed form solution is available for this problem (note that this is different from the problem of standard catheters [7], [15]). An optimization procedures, for instance a Gauss-Newton algorithm using the inverse of the jacobian

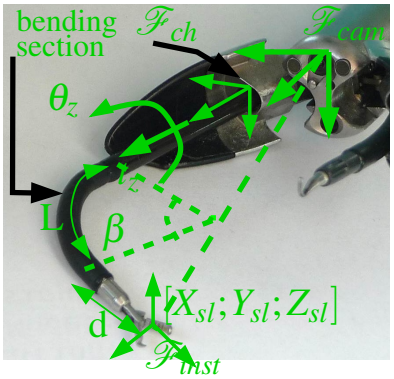

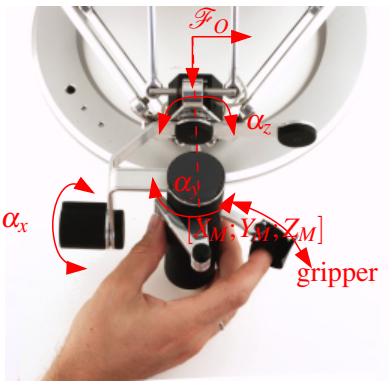

Fig. 2. Distal extremity of the slave system (left) and one master interface (right) with their associated frames and DoFs.

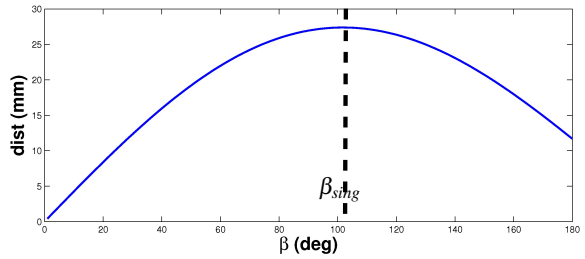

Fig. 3. Evolution of the distance of the tip of the instrument to the axis of rotation in function of deflection angle.

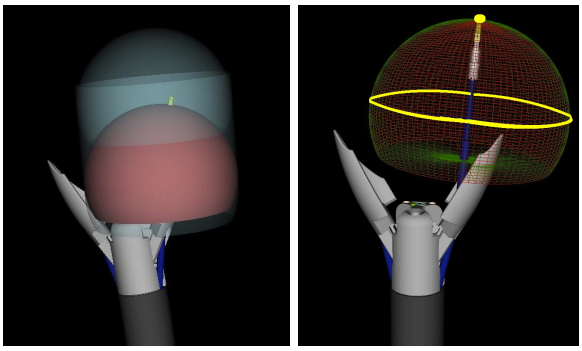

Fig. 4. Workspace of the right instrument (left) and local workspace spanned by deflection and rotation. The yellow line corresponds to the singularity at β_{sing} and the yellow ball to the singularity at $\beta = 0$.

[7], could be used for finding one solution. However, for obtaining all possible solutions we solve it the following way. First the desired cartesian position ${}^{cam}P^*$ is expressed in frame $\mathscr{F}_{ch}$: ${}^{ch}P^* = (X^*, Y^*, Z^*)$. The distance of the point to the axis ${}^{ch}z$ can be expressed as $dist = \sqrt{Y^{*2} + X^{*2}} = \left|\frac{L}{\beta}(1 - cos(\beta)) + dsin(\beta)\right|$. As shown on Fig. 3, there are generally two positive solutions β^*_{1+} and β^*_{2+}, one on each side of the singularity, and their opposite negative solutions. The solutions can be found by using golden-section search. The rotations are computed as $\theta^*_{z+} = atan2(Y^*, X^*)$ and $\theta^*_{z-} = \theta^*_{z+} + \pi$. Finally, one obtains t_z from equation (1), as $t_{z1,2} = Z^* - \frac{L}{\beta^*_{1,2}} sin(\beta^*_{1,2}) - dcos(\beta^*_{1,2})$.

If not considering workspace limits in deflection and rotation, there is therefore a four-fold discrete redundancy in position:

- by inverting both deflection and rotation: this results in a rotation of 180^o of the effector;
- by using β values on each side of β_{sing}. The point can therefore be reached with two different orientations, either directly ($|\beta| < |\beta_{sing}|$) or "from behind" ($|\beta| > |\beta_{sing}|$).

D. Workspace

Deflection and rotation span an almost ellipsoidal surface. Combined with the translation this creates a cylinder whose axis is defined by ${}^{ch}z$, the direction of the flap at the extremity of the endoscope and with ellipsoidal head and tail defined by the limits in translation (see Fig. 4).

Deflection can vary from $-120°$ to $120°$. Practically, for not twisting electrical cables at the back of the modules handling translation and rotation, the rotation is limited to $[-170°; 170°]$ by mechanical end stops. With these ranges all points in the truncated cylinder can be reached with at least one orientation. Most can be reached at least with two opposite orientations. Some, lying at the most external part of the cylinder can be reached with four orientations.

III. Master / Slave Control

A. Control overview

The slave robot is controlled at the joint level only by a position loop running at 1000 Hz on a central controller. As stated before, no high-level techniques have been used to reduce nonlinear effects due to the cable actuation of the deflection.

For now the master side consists of two commercial interfaces (omega.7 from Force Dimension) and a pedal board (2 monostable pedals). The omega.7 has 7 DoFs (q_M): the cartesian position of the handle (X_M, Y_M, Z_M), which is actuated and allows force feedback, the rotation of the handle $(\alpha_x, \alpha_y, \alpha_z$, passive DoFs) and a gripper. Since there is no force measurement on the slave side, all force effects on the master side are only used to artificially constrain or guide the gestures of the user.

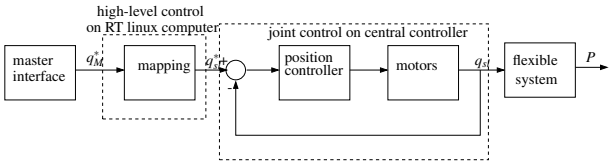

Fig. 5. Master/slave control principle for one instrument

slave DoFs	t_z	θ_z	β	X_{sl}	Y_{sl}	Z_{sl}	grasper
joint control	Z_M	α_z	gripper				pedal
orientation guid.	$\int Z_M$	α_z	$\pm\sqrt{X_M^2+Y_M^2}$				gripper
pseudo-cart.	Z_M	$atan2(Y_M,X_M)$ $(+\pi)$	$\pm\sqrt{X_M^2+Y_M^2}$				gripper
cartesian				X_M	Y_M	Z_M	gripper

TABLE I

CONSIDERED MAPPINGS BETWEEN MASTER INTERFACES AND SLAVE INSTRUMENTS. FOR SAKE OF CLARITY SCALE FACTORS HAVE BEEN OMITTED. $\int$ DENOTES CONTROL IN VELOCITY.

The master interfaces have more or less a hemispheric workspace for the position of the handle. Rotation α_z is limited to $[-135°;135°]$. The gripper has a $50°$ range (about $48mm$ of linear motion). Other rotations are not used in our developments.

A high level controller running on a computer under a real-time linux OS communicates with the master interfaces and provides reference joint positions to the slave central controller (see Fig. 5).

B. Proposed control modalities

The two master interfaces are used to control the two instruments. One of them can be chosen to alternatively control the endoscope: by pressing the left pedal of the pedal board, the control from the chosen interface is transferred to the endoscope.

Several control modalities have been proposed for the instruments. For all modalities absolute mappings are used between the master interfaces and the instruments. Scaling has been used to provide maximum slave to master motion amplification, except for rotation α_z (when used), which is directly mapped onto θ_z without scaling. This manner, there is no need to engage/disengage a clutch during the manipulation of the instruments. This approach allows immediate control of the instruments with the largest possible master-to-slave downscaling.

To combine easy switching from instrument to endoscope with instrument absolute mapping, we have decided to control the endoscope in velocity as explained in [4].

The differences between the control modalities arise in the way the instruments are controlled. Here we describe the different proposed mappings (see also table I) and the force effects used for constraining motions, when applicable.

a) **Joint Control***:* In this modality each joint of the slave system is controlled separately by an elementary motion of the master interface. We have taken advantage of the mechanical architecture of the omega.7 to propose a master control very similar to the available DoFs of the instruments. The rotation axis α_z of the handle controls the rotation of the instrument. The gripper (motion of the index finger) of the master interface controls the deflection of the instrument. Because the range of the gripper is limited, it has been chosen to map it on the positive deflections only. The translation of the instrument t_z is defined by the position of the handle along Z_M. Grasper opening / closing is controlled by pressing the right pedal. The position of the handle in the (X_M,Y_M) plane is not used, hence a force effect is applied to limit unwanted motions in this plane. The physical range of α_z is included in the feasible range of θ_z, which slightly limits the reachable workspace (see Fig. 6).

b) **Orientation guidance***:* This modality is also a kind of joint control. The orientation α_z of the handle defines the rotation of the instrument as in joint control. The deflection of the instrument is then controlled by translating the handle in the X_MY_M plane. This motion is constrained along a straight line by a force effect, so that the gripper on the master interface keeps the same orientation as the instrument. The range of motion is sufficient to map both positive and negative deflections. Moreover, the gripper of the master interface can be used for controlling opening and closing of the instrument grasper. Uniform force effects are suitable for constraining the motion of the handle. This is more easily achieved with our master interface if the position of the handle along axis Z_M remains constant. This is obtained by controlling the translation in velocity along Z_M. This motion is damped by a force effect, so that the handle always remains in the neighborhood of $Z_M = 0$.

c) **Cartesian control***:* This modality allows to directly control the position (X_{sl},Y_{sl},Z_{sl}) of the tip of the instrument in the frame $\mathscr{F}_{cam}$ with the cartesian position of the master interface (X_M,Y_M,Z_M). The inverse position kinematic of the system is used to compute the desired joint positions.

d) **Pseudo-Cartesian control***:* In this modality the deflection of the instrument is controlled by the distance of the handle of the master interface w.r.t. the central position in the X_MY_M plane. The angle of rotation is obtained as $\theta_z = atan2(Y_M,X_M)$, and the position Z_M of the interface directly controls the translation t_z of the instrument. The rotation of the handle has no effect on the slave system. The interface gripper controls the opening and closing of the grasper of the instrument. This modality provides an approximate sense of cartesian control. Indeed, the relative motions of the handle performed on the master side are approximately reproduced on the slave system. The absence of depth perception for the user tends to reinforce this feeling.

IV. INSIGHTS INTO CARTESIAN CONTROL

This section provides additional explanations for cartesian and pseudo-cartesian control.

A. Limitations in rotation

For cartesian and pseudo-cartesian modalities it is necessary to warn the user that the slave system is blocked by end-stops in rotation, otherwise the user might reinforce his motion in the absence of visible reaction of the slave system. We have chosen to use a force effect on the master interface,

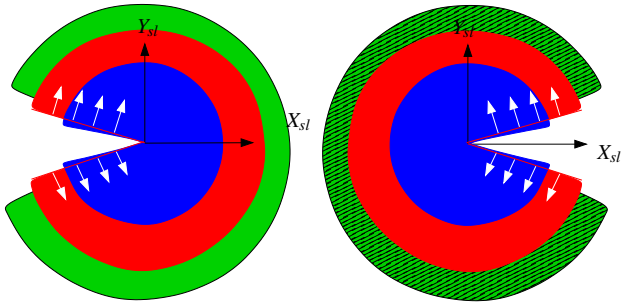

Fig. 6. XY workspaces for negative (left) and positive (right) deflections (represented for the right instrument). Slave workspace (blue) and master workspace mapped to the slave level for joint control (hatching), orientation guidance (green), and for cartesian and pseudo-cartesian (red). White arrows indicate the force effects on the master interface for cartesian and pseudo-cartesian modalities. The radius of the master workspace can be tuned by scaling factors. The displayed radii are not representative and have been chosen for readability only.

which pushes the handle toward the free workspace and prevents the user to enter in the restricted area (see Fig. 6). This effect appears when $\theta_z = atan2(Y_M, X_M) \in [-20°; 20°]$ for $\beta \geq 0$ (*i.e.* on the right of the master workspace for the right master interface), and when $\theta_z = atan2(Y_M, X_M) + \pi \in [160°; 200°]$ for $\beta < 0$ (*i.e.* on the left of the master workspace for the right master interface).

B. Handling singularities and redundancy

Singularities in position have to be handled in cartesian and pseudo-cartesian control. For now, the deflection has been voluntary limited to $|\beta| \leq 90° \leq \beta_{sing}$ because the available workspace beyond β_{sing} is very small. Therefore it did not seem interesting to handle this singularity for a very little benefit.

However, in these control modalities the rotation of the instrument is obtained from the (X_M, Y_M) position through $\theta_z = atan2(Y_M, X_M)$. Tremor and noise on the master interface can create uncontrolled rotations of the instrument near the straight configuration. Conversely, the rotation, which can be modified freely in the straight position in joint control modalities, cannot be directly controlled with the available DoFs of the master interface. Also, around singularities the choice of the solution for the inverse of the position kinematic model can be difficult because it requires to understand what the user wants to do.

A simple solution could consist in blocking deflection to $|\beta| > \beta_{min}$, but this would create a hole in the position workspace.

Another solution could consist in blocking the rotation around the straight configuration for avoiding unwanted rotations. The drawback is that in the blocked area it is not possible to change the direction of motion anymore, and changes applied at the master side are only applied once the deflection becomes greater than β_{min}, creating a potentially disturbing rotation of the instrument.

We have proposed a solution consisting in subtracting a small offset $\beta_{off} < 0$ on the deflection axis combined with blocking the rotation for $\beta < \beta_{off}$. For instance, for pseudo-cartesian modality, the deflection of the slave system is now computed as $\beta = \lambda \sqrt{X_M^2 + Y_M^2} - \beta_{off}$, where λ is the master to slave scale factor. As a result, the straight position can now be reached with the master interface on a circle of radius $\frac{\beta_{off}}{\lambda}$. Moreover, the rotation of the instrument can be controlled by moving on this circle, with $\theta_z = atan2(Y_M, X_M)$. If the user enters inside the circle, the deflection becomes slightly negative. For avoiding the singularity and associated uncontrolled rotations, the rotation inside the circle is blocked to its value at the time the circle has been entered.

For non symmetric instruments, such as hooks or knifes it can be interesting to use the redundancy provided by negative deflection. This redundancy also allows to change the position of the rotation limits in the XY plane (see Fig. 6). This means that a choice has to be made between positive and negative deflections when solving the inverse position kinematic. The switching from positive to negative deflections should occur while the deflection is null for avoiding discontinuities. Therefore, we propose to change the sign of the deflection inside the rotation blocking area, once the center of the circle has been crossed. As mentioned before, with the proposed technique the deflection is negative once the user has entered the circle. Switching thus makes deflection go from $-\beta_{off}$ to β_{off} which should create a discontinuity on the slave side. However, when changing deflection direction, the discontinuity is largely, if not completely, absorbed by backlash. Note that at the time of switching the offset and the restricted area for the handle must also be inverted.

C. Parameters tuning

β_{off} has to be chosen larger that the amplitude of noise and / or tremor affecting the master interface, which could otherwise create uncontrolled rotations of the instrument. It should also be sufficiently large to allow the user to easily switch from positive to negative deflection. On the other hand β_{off} tends to deform the mapping of master trajectories to the slave trajectories. Also, if the rotation-blocking circle is too large it can happen that deflection is switched while this is not desired. On our system we have empirically tuned $\beta_{off} = 20°$ which corresponds to a circle of radius 3cm on the master side.

D. Graphical interface

For assisting the user in cartesian and pseudo-cartesian modalities, two windows are displayed on a side screen, which show the current positions of the master interfaces with respect to the rotation blocking area and the deflection switching limit as well as the position of rotation end stops (see fig. 7). This interface could be replaced by visual or sound alarms for decreasing the required cognitive load.

V. Experimental results

In this work, we have wished to focus on the use of a single instrument, in order to assess the effects of non-linearities on the different approaches. Although in real

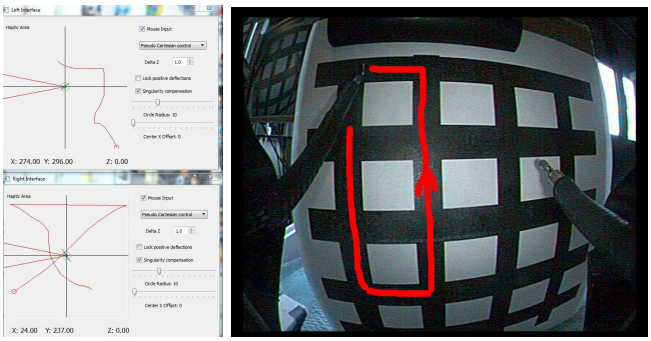

Fig. 7. Left: Windows displaying the position of the interfaces with respect to rotation limits (red lines), rotation blocking circle (green circle) and deflection switching limit (blue line) for cartesian and pseudo-cartesian modalities. Right: Snapshot from the endoscopic images, as seen by the user during task 1. The path (indicated in red) has to be followed using the left instrument only. The path goes through the straight configuration and reach the limit of the instrument workspace (top and bottom).

surgical conditions the surgeon will position the endoscope in order to facilitate manipulation with the instruments, it is still important that instruments could be controlled easily in a wide workspace, so as to avoid frequent repositioning of the scope and to allow tasks involving the use of both instruments in different working areas. Moreover, in some intraluminal procedures the limited space can prevent or limit endoscope repositioning.

A. Experiments

For comparing the selected control modalities, we have developed a testbed with three tasks. Our objective is to objectively compare the possibilities of the different modalities in terms of accuracy and reactivity.

Task 1: It consists in following a path in the image with the tip of the instrument (see Fig. 7). It is aimed at assessing the accuracy in trajectory following, independently of depth perception difficulties. The duration for performing the task is measured as well as the number of errors, *i.e.* when the instrument goes out of the reference trajectory.

Tasks 2 and 3: These tasks consist in successively pointing four points. The trajectory between points is free. For task 2, pointing is done in the image plane only, while for task 3 the tip of the instrument must be brought inside holes. This task is aimed at assessing the ease of pointing, *i.e.* switching from large and fast motions to accurate and fine positioning.

The proposed tasks include challenging motions or positions, at the extremity of the workspace, near the straight configuration and near the mechanical limits of the rotation. While they are not directly representative of surgical procedures, pointing and trajectory following are necessary in most procedures, for instance in Endoscopic Submucosal Dissection using electrosurgical instruments. Three users familiar with the manipulation of the robotic system have been requested to successively perform the tasks with all modalities. For each modality the user could train on a neutral environment.

B. Analysis and discussion

Results for task durations are reported on Fig. 8, where the durations for each user, each task and each modality are expressed in percentage of the duration obtained for the same task and the same user using joint control.

It appeared that the line following task is very difficult, for every modality, even for users familiar with the system. The number of errors for all users and all modalities is important (between 4 and 8), with two kinds of excursions outside the path: slight deviations (a few millimeters) and large motions (more than one centimeter). Small deviations are due to: 1) Difficulties to track the trajectory. For joint control strategies this comes from the unnatural coordination of motions that the user has to figure out. For cartesian strategies they are due to non-linearities, which create erroneous coordinations of deflection and other axes; 2) To uncontrolled rotation motions of the instrument near the straight singularity (cartesian and pseudo-cartesian). Large motions outside the path arise for the following reasons: 3) The limit of the workspace has been reached and a reconfiguration is required to continue moving along the path (all modalities); 4) Non-linearities create large uncontrolled motions (cartesian modality); 5) The user loses control of the instrument because he has gone beyond the force wall effect (cartesian and pseudo-cartesian).

Pointing tasks are accomplished more easily, since reaching workspace limits and reconfigurations between targets do not penalize the success of the task too much.

For all tasks and for all users, orientation guidance increases task duration with respect to direct joint control. Orientation guidance had originally been proposed to avoid two identified limitations of direct joint control: the sensitivity of deflection control and the need to use a pedal for closing the grasper. It seems that unfortunately the axis mapping is less intuitive. Moreover the use of force effects to constrain the gesture is not optimal.

Comparisons between cartesian and pseudo-cartesian modalities (with and without negative deflections) show that pseudo-cartesian allows better control. For the cartesian modality the singularity at the limit of the workspace (near β_{sing}) implies that when the user modifies X_M or Y_M around the limit of the workspace large changes appear on β which are compensated by large velocities along t_z. Because of non-linearities on the deflection, there is no exact coordination of β and t_z, which results in large unwanted motions when the instrument has an important deflection. For pseudo-cartesian modality there is no such singularity at the limit of the workspace because t_z is controlled separately.

Comparison between the use of positive deflection only and the use of positive and negative deflections shows that the possibility to switch does not really improve gesture. The proposed tasks did not require specific orientation. Therefore switching was mainly interesting for avoiding workspace limits. However, undesired switching frequently happens, which then brings the instrument near workspace limits and hinder the continuation of the task.

Results for joint control and pseudo-cartesian control are close in terms of task duration and tracking errors. The

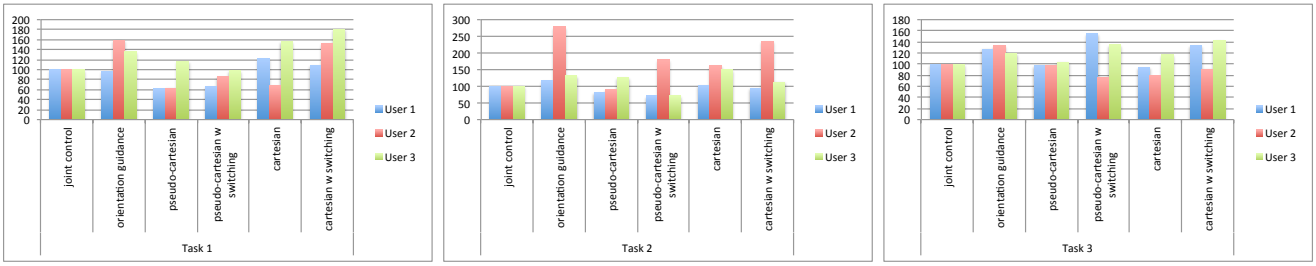

Fig. 8. Tasks durations in percentage of the duration of the same task realized by the same user with joint control.

difficulties are however different. For joint control they mainly come from the difficulty to synchronize axes motions for creating a desired operational movement. For the pseudo-cartesian modality the limitations in accuracy are due to non-linearities which create unwanted motion directions. Two shortcomings have also been identified. Because of inaccurate estimation of the straight configuration, the rotation can be blocked far away from the real straight configuration. Despite force effects, it happens that the user passes through the virtual limits on the master side. The instrument does not move anymore and the user loses track of the control.

Both joint control and pseudo-cartesian modalities could benefit from backlash compensation. For joint control it would decrease sensitivity between master and slave for the deflection. For pseudo-cartesian it would improve accuracy for small motions.

VI. Conclusion

In this paper we have proposed several master/slave mappings for controlling the instruments of our flexible robot, STRAS, with commercial interfaces omega.7. No external sensors were used and the user was in charge to close the operational loop. As expected, non linearities in the deflection of the instruments disturb the user when performing accurate trajectory following tasks. This is especially an issue for cartesian control. However, the proposed pseudo-cartesian modality, which decouples depth control from other axes allow to obtain similar accuracy results as standard joint control, while requiring lower concentration level from the user. This analysis is of interest for systems combining standard master interfaces and "catheter-like" slave systems. Nevertheless, improvements are needed to allow better experience for the user. Non-linearity compensation as well as a way to accurately estimate straight positions of the instruments would be useful, but this would require the use of an external sensor. On the master side, the development of a specific interface with adapted mechanical end stops could also improve the mapping between master and slave.

References

[1] C. Thompson, M. Ryou, N. Soper, E. Hungess, R. Rothstein, and L. Swanström, "Evaluation of a manually driven, multitasking platform for complex endoluminal and natural orifice transluminal endoscopic surgery applications," *Gastrointestinal Endoscopy*, vol. 70, no. 1, pp. 121–125, July 2009.

[2] L. L. Swanström, R. Kozarek, P. J. Pasricha, S. Gross, D. Birkett, P. O. Park, V. Saadat, R. Ewers, and P. Swain, "Development of a new access device for transgastric surgery," *Journal of Gastrointestinal Surgery*, no. 9, pp. 1129–1137, 2005.

[3] S. J. Phee, S. C. Low, V. A. Huynh, A. P. Kencana, Z. L. Sun, and K. Yang, "Master and slave transluminal endoscopic robot (MASTER) for natural orifice transluminal endoscopic surgery (NOTES)," in *IEEE International Conference on Engineering in Medicine and Biology*, Minneapolis, USA, 2009, pp. 1192–1195.

[4] A. D. Donno, L. Zorn, P. Zanne, F. Nageotte, and M. de Mathelin, "Introducing STRAS: a new flexible robotic system for minimally invasive surgery," in *IEEE International Conference on Robotics and Automation*, Karlsruhe, May 2013.

[5] V. Agrawal, W. J. Peine, and B. Yao, "Modeling of transmission characteristics across a cable-conduit system," *IEEE Transactions on Robotics*, pp. 914–924, 2010.

[6] J. Jung, R. Penning, N. Ferrier, and M. Zinn, "Modeling approach for continuum robotic manipulators: Effects of nonlinear internal device friction," in *IEEE / RSJ International Conference on Intelligent Robots and Systems*, San Francisco, September 2011, pp. 5139–5146.

[7] R. J. Webster III and B. Jones, "Design and kinematic modeling of constant curvature continuum robots: A review," *International Journal of Robotics Research*, vol. 29, no. 13, pp. 1661–1683, June 2010.

[8] R. Penning, J. Jung, B. J., N. Ferrier, and M. Zinn, "Towards closed loop control of a continuum robotic manipulator for medical applications," in *IEEE Int. Conf. on Intelligent Robots and Systems*, 2011, pp. 4822–4827.

[9] R. Reilink, S. Stramigioli, and S. Misra, "Pose reconstruction of flexible instruments from endoscopic images using markers," in *IEEE International Conference on Robotics and Automation*, Saint Paul, USA, 2012, pp. 2938–2943.

[10] B. Bardou, F. Nageotte, P. Zanne, and M. de Mathelin, "Improvements in the control of a flexible endoscopic system," in *IEEE International Conference on Robotics and Automation*, Saint Paul, USA, 2012, pp. 3725–3732.

[11] K. Xu and N. Simaan, "Actuation compensation for flexible surgical snake-like robots with redundant remote actuation," in *IEEE International Conference on Robotics and Automation*, Orlando, Florida, May 2006, pp. 4148–4154.

[12] V. Agrawal, W. Peine, and B. Yao, "Dual loop control of cable-conduit acuated devices," in *American Control Conference*, Montreal, 2012, pp. 2621–2626.

[13] A. Bajo, R. Goldman, L. Wang, D. Fowler, and N. Simaan, "Integration and preliminary evaluation of an Insertable Robotic Effectors Platform for Single Port Access surgery," in *IEEE International Conference on Robotics and Automation*, St Paul, USA, 2012, pp. 3381–3387.

[14] K. Ikuta, T. Hasegawa, and S. Daifu, "Hyper redundant miniature manipulator " hyper finger " for remote minimally invasive surgery in deep area," in *IEEE International Conference on Robotics and Automation*, 2003, pp. 1098–1102.

[15] S. Neppalli, M. A. Csencsits, B. A. Jones, and I. D. Walker, "Closed-form inverse kinematics for continuum manipulators," *Advanced Robotics*, vol. 23, pp. 2077–2091, 2009.